A STUDY OF 15-20 GEV MASSIVE MUON PAIRS

Columbia-Fermilab-Stony Brook Collaboration

Introduction

E288 made a precision measurement of 5-15 GeV mass muon pairs produced in 400 GeV proton-nucleon collisions. The data yielded many exciting insights into the nature of the interactions of the constituents of hadrons. Both the discovery of the upsilon family and the careful measurement of the continuum of massive muon pairs have guided those who wish to describe the interactions of quarks and gluons in hadrons. It is clear that virtual photons are an important tool for probing hadron constituents and such studies should be pushed to the kinematic limit of the Fermilab accelerator.

The recent high intensity phase of E288 represented the best that could be done with the current experimental apparatus available in the P-Center experimental area. We have turned our attention to designing an apparatus with higher luminosity and acceptance in order to explore the mass range from 15 to 20 GeV. This proposal outlines an apparatus which will be capable of reaching these goals in 4000 hours of running at $> 10^{13}$ incident protons per pulse. An important design criteria is the expected resolution of 0.7% which should allow the clean observation of the top quark if its mass is less than 11 GeV. With the advent of 1000 GeV protons, the mass sensitivity extends to 28 GeV, or 15 GeV top quarks!

Apparatus

In order to increase both the resolution and luminosity at higher masses it is necessary to increase the magnetic bending available. We propose to incorporate in our design the large charged hyperon production magnet (with modified pole tips) that will be used in P-Center for E497. We also propose to add another magnet of similar construction to achieve a total transverse magnetic kick of almost 10 GeV/c. This enables us to construct a classic mass focusing spectrometer in the style long associated with neutral kaon spectrometers. Muon pairs of 20 GeV mass exit these two magnets approximately parallel to the initial beam direction (see Fig. 1) allowing a fairly compact apparatus transversely and also added room for shielding. The design and cost estimate of the second magnet is given in Table I, the estimate was based on construction techniques similar to those being employed in the present hyperon dump magnet construction.

The MWPC's and the counter hodoscopes are quite similar to those being used in E288. Indeed some of the dimensions have been chosen to allow reusing, with different mounting, some of the MWPC's and scintillation counters of E288.

The large solid steel magnet M3 allows the redetermination of the muon momentum to ±10% and hence rejection of events originating from the beam dump. It will again be a modification of the existing steel magnet in E288.

Sensitivity Estimates

The muon pair acceptance at the mass to which the magnetic field is tuned will be 3%, four times bigger than our present 0.8%. This estimate is based on a Monte Carlo study which incorporates our current measurements of the 10-15 GeV mass spectrum folded into a Drell-Yan model. Our current apparatus can handle 8×10^{11} protons per pulse. A conservative estimate of the effect of the extra shielding, the factor of 8 increase in magnetic bending, the smaller solid angle of the detectors, and the location of all sources of background in a large uniform magnetic field leads us to expect an operating intensity of $\gtrsim 10^{13}$ protons per pulse. The expected resolution, dominated by the 220" of Be in the first magnet, is 0.7%. This is a factor of 3 better than the high intensity version of E288 and a factor of 2 better than the current high resolution stage of E288. The sensitivity of this apparatus should be an overall factor of

$$\frac{3.0\%}{0.8\%} \text{ acceptance } \times \frac{10^{13}}{8 \times 10^{11}} \frac{\text{protons}}{\text{pulse}} = 50$$

higher than E288. If we add the improvement in resolution relevant to bump hunting in a (conservatively) linear way, the gain is 150. The mass acceptance of the apparatus is reasonably narrow, see Fig. 2, necessitating more than one setting to cover the spectrum from the upsilon region up to the highest masses attainable. We assume that about one-half the running time will be used at the highest

setting giving therefore a real factor of about 25 increase over E288. We are convinced triggering will present no problems as the mass focusing coupled with simple matrix logic selection on the three banks of hodoscope trigger counters T_1, T_2 and T_3 (as we currently do in E288) will give very low trigger rates. We found in E288 that the first few tune-up runs uncover the origin of spurious triggers and yield an optimum matrixing strategy.

Acceptance Details

The proposed arrangement greatly improves the Feynman-x acceptance range over E288 (the factor of 3%/0.8% contains this) as well as an improved acceptance in $\cos\theta^*$. Thus, we enter the new mass domain with apparatus which will be far more incisive in so far as continuum studies are concerned. There is also a modest improvement in the P_T acceptance.

Estimate of Running Time

In the high intensity version of E288 we have 50 events in the 14-15 GeV mass bin from 1000 hours of running. The yield of massive pairs is falling exponentially with mass

$$S \left.\frac{d^2\sigma}{d\sqrt{\tau}\, dy}\right|_{y=0} = 0.45 \exp(-25.5\sqrt{\tau})$$ [1]

$$\tau = m_{\mu^+\mu^-}^2/S$$

[1] J. K. Yoh et al., Study of Scaling in Hadronic Production of Dimuons, to be published.

Thus, to obtain the same number of events in a bin from 19-20 GeV (remember the resolution is better) will require

$$1000 \text{ hrs} \times \exp(-25.5\ (20 \text{ GeV} - 15 \text{ GeV})/27.4) \div 50 \text{ (improvement)}$$

$$= 2000 \text{ hours.}$$

The mass acceptance is such that we will obtain the following data (continuum only):

Mass	Events
>20	~ 10
19-20	50
18-19	120
17-18	250
16-17	500
15-16	1000
14-15	~ 1000
13-14	$\sim$ 200?

Tuning and data taking at lower mass settings should consume another 2000 hours. An upsilon-strength signal at 20 GeV would yield 40 extra events in a 300 MeV bin in which 12 would be expected. A $t\bar{t}$ state (charge +2/3) would be better by a factor of 4.

Doubler

Since the apparatus tilts towards forward angles, we would be completely compatable with 1 TeV running, indeed the extension of the mass search beyond 20 GeV is a basic motivation of this approach. A 1 TeV configuration would involve moving the target and beam dump upstream to allow the use of the full magnetic length of the hyperon dump magnet after a consequent modification of the pole inserts. Because the laboratory angles of the produced muon pair fold forward as the ratio $\sqrt{1000/400}$ we would obtain a larger acceptance in this modified arrangement. Therefore, the table above can be roughly translated such that 19 GeV$\rightarrow \lesssim$ 28 GeV. We note that we now reach close to the limit of the PEP-PETRA "competition".

Time Scale

The magnet steel and coil acquisition and construction will be the longest and costliest item. We would expect that the magnet would be ready to install by the end of 1979 which should coincide with the end of the charged hyperon experiment in P-Center. We would have the necessary MWPC and trigger counter construction and modifications completed and would be ready to install at that time.

μμ III Second Magnet

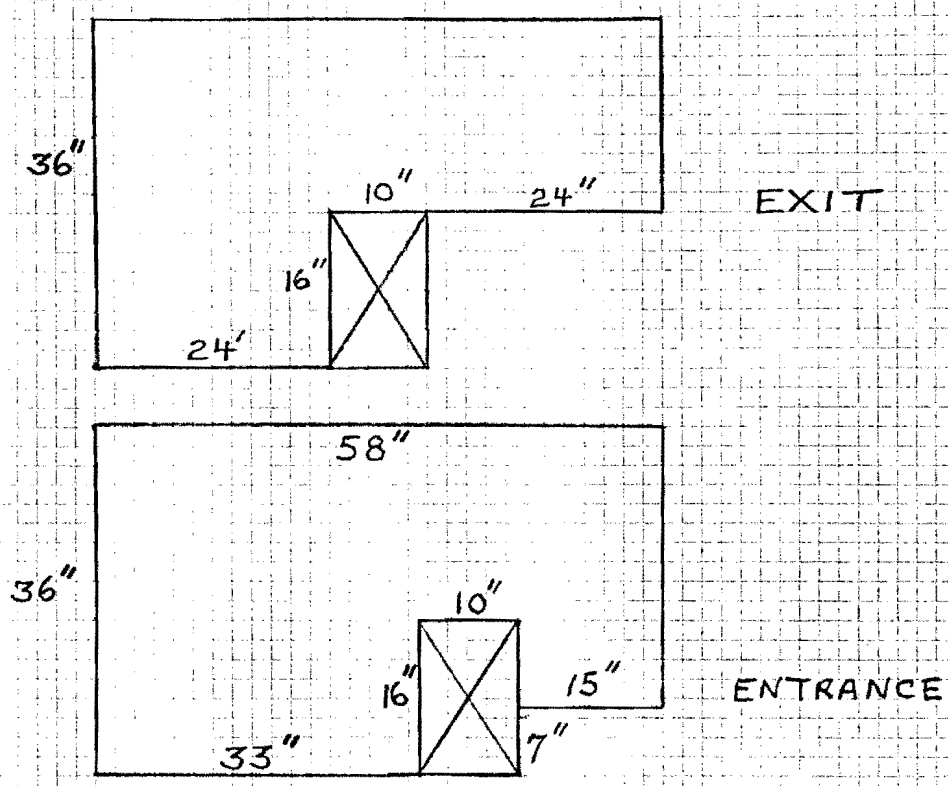

End View of One Quadrant

TABLE 1.

B entrance	24 KG.
B exit	10 KG.
$\int B \cdot dl$	4 GeV/c.
Length	8 meters
Power	1.2 MW
Weight Cu.	55,000 lbs.
Weight Fe.	350 TONS
Amp-Turns	625,000
Cost	Cu 280 K
	Fe 120 K
	Fixtures 100 K
	Contingency 100 K
	500 K

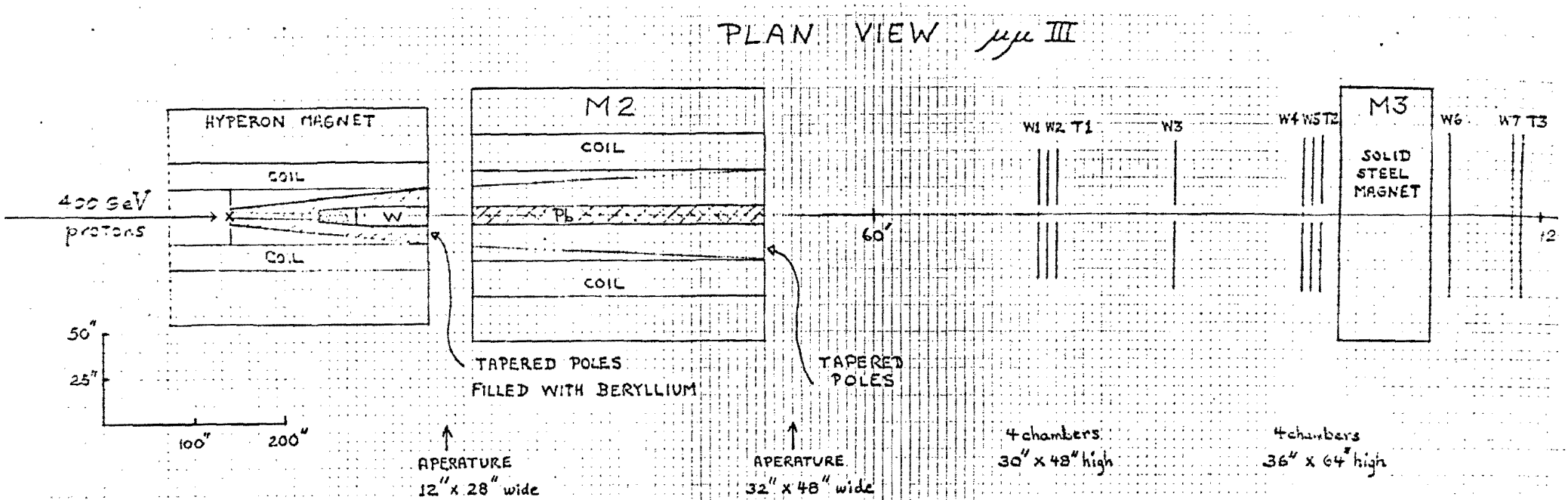
PLAN VIEW μμ III
HYPERON MAGNET
COIL
W
COIL
400 GeV
protons
50"
25"
100"
200"
M2
COIL
Pb
COIL
TAPERED POLES
FILLED WITH BERYLLIUM
APERATURE
12" x 28" wide
TAPERED
POLES
APERATURE
32" x 48" wide
60"
W1 W2 T1
W3
4 chambers
30" x 48" high
W4 W5 T2
M3
SOLID
STEEL
MAGNET
4 chambers
36" x 64" high
W6
W7 T3
12

Figure 1.

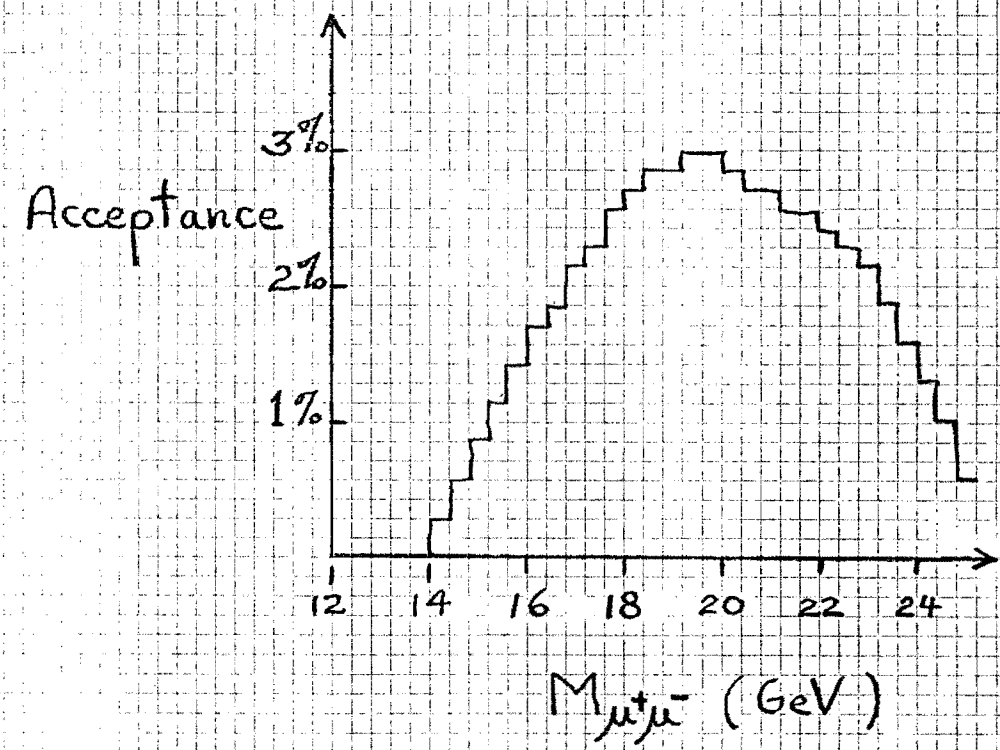

Monte Carlo generated (model tailored to fit E288 data).

Figure 2.

Addendum to Proposal 605

STUDY OF LEPTONS AND HADRONS NEAR THE KINEMATIC LIMITS

L. M. Lederman and W. Sippach
Columbia University
New York, New York 10027

and

B. C. Brown, C. N. Brown, R. Dixon
K. Ueno, and T. Yamanouchi
Fermi National Accelerator Laboratory
Batavia, Illinois 60510

and

G. Charpak and F. Sauli
CEN, Saclay
France

and

G. Coutrakon, D. A. Finley, A. S. Ito,
H. Jostlein, and R. L. Mc Carthy
State University of New York at Stony Brook
Stony Brook, New York 11794

We specify here some details of our proposal in addition to those given in our earlier communications.[1,2] We feel that we have succeeded in merging the physics objectives of proposals 605 and 586. We now propose to run the experiment without the beryllium hadron absorber in its initial configuration. We also propose to use a cyclotron magnet for the second momentum measurement and have changed the chamber configuration.

CONTENTS

ADDENDA

		Page
I.	Support Requested	3
II.	Physics Goals	3
III.	Configuration	4
IV.	Scope of Measurements	10

APPENDICES

I.	Nevis Cyclotron	20
II.	Chambers	22
III.	Lead-Glass Calorimeter	23
IV.	Hadron Calorimeters	24
V.	Hadron Species Identification	25
VI.	Radiation	34
VII.	Details of Calculations	36
VIII.	Trigger	40
IX.	Competition	46
X.	Impact of the Tevatron	47

SUPPORT REQUESTED

We request 4000 hours of running time (tuning included) in the phase 1 configuration outlined below. The magnets required represent a major investment for Fermilab and have a fairly long lead time.

PHYSICS GOALS

(1) Search for new high mass dilepton resonances. (See Ref. 1, 2.)

(2) Study the structure of hadrons. (See Ref. 1,2.)

We plan to simultaneously detect hadrons and leptons, both singles and +/- pairs, nearly out to the kinematic limits. Extrapolations from present data indicate that we should be able to reach regions ($x_T > 0.9$ for singles $\sqrt{\tau} > 0.8$ for pairs) where the ratio of direct Drell-Yan dileptons to hadrons should increase if present trends continue. Such an observation would amount to verification that hadrons are produced only indirectly - by the decay of directly produced constituents. In this region, then, we hope to suppress kinematically the usual hadronic debris and study direct constituent interactions in hadronic collisions. Such data would complement well the progress which has recently been made with leptonic probes. We enter this new, uncharted region with the opportunity to make decisive first measurements, whatever we may find.

(3) Test μ- e universality. (See Ref. 2.)

We should be able to reach timelike $Q^2 \sim 300$ $(GeV/c)^2$ with good sensitivity to differences in shape (bumps) between the dimuon and dielectron mass spectra. The muon must have structural differences from the electron because of its mass. Using our deep virtual photon probe, we hope to uncover the nature of these differences.

CONFIGURATION

Phase 1 is a minimal, no-frills configuration which we feel, nevertheless, will allow us to do some very exciting physics and justifies by itself the considerable support we are requesting. We label as "phase 2" those aspects of our program which involve

(1) untested technology (high resolution chambers, hadron species identification)

(2) the super M1 pion beam

(3) a hydrogen target (The most interesting uses of a hydrogen target involve the pion beam.)

In the case of untested technology, we will attempt now to begin building and testing the necessary prototypes so that this technology may actually be used in the initial running, if possible. We will inform the PAC when the technology has been successfully developed.

Magnets. (See Ref. 1.)

M1 and M2 together provide a p_t kick of up to ~10 GeV/c, and hence focus onto our detectors pairs with masses ~20 GeV/c. These magnets also provide a clean shield against low p_T background.

We now request that M3 be a large air-gap magnet (see Appendix I) for the following reasons.

(1) This allows simultaneous detection of μ, e hadrons out to the kinematic limit. The systematic control provided by a 3% remeasurement of a particle's momentum (phase 2: 0.9%) should allow our measurements to be free of background even at the kinematic limit for single particles.

(2) We now feel that the solid steel magnet remeasurement scheme outlined earlier (Ref. 1.) is marginal for clean separation of dimuons originating in the dump from those originating in the target. If two muons, originating at the dump and target respectively, have identical trajectories at a given detector, their momenta must differ by at least 30%. The previous scheme (resolution 12%) is insufficient in the presence of steeply falling cross sections and non-Gaussian tails on the momentum resolution function.

Luminosity

Our detection apparatus (Fig. 1) is shielded against neutrals from the target by the dump which subtends horizontal production angles of ±40 mr. This arrangement is particularly clean because neutrals cannot exit M2. The particles we accept are bent around the dump and into our acceptance. The dump (Appendix VI) is planned to be a 3m long water-cooled copper block (20 interaction lengths) filled with a 1 inch radius tungsten plug (30 interaction lengths) on the beam axis. We shield ourselves from the back of the dump

with a uniform wall of magnetic field (4 GeV/c kick) followed by an 8m drift space. Extrapolating our previous experience, this geometry should allow very few spurious tracks and we feel that we can operate, even without the beryllium absorber at 10^{13} incident protons/pulse. We presume here, however, an incident intensity of 3×10^{12}, without absorber, in order to lessen our burden on the accelerator.

Hadron Absorber.

We now propose to run initially without the beryllium hadron absorber.[1] If our attempts to run without absorber are successful, we will receive the following benefits:

(1) simultaneous detection of μ, e, hadrons

(2) improvement of the mass resolution by a factor of 3 to 8!

Because of this improved resolution, we hope to increase our sensitivity to high mass dilepton resonances by taking out the beryllium. Making the somewhat pessimistic assumption that

$$\text{sensitivity} \sim (\text{intensity/resolution})^{1/2}$$

we can turn down our intensity by a factor of 3 with no absorber and still increase our sensitivity by a factor of 2 to 5 (remembering we will collect dielectrons as well as dimuons).

We are encouraged to attempt running without absorber by our extremely clean geometry and by the fact that the hadron/lepton ratio is expected to decrease at high x_T (Fig. 2). If we

are unsuccessful in this attempt to run at high intensity without absorber, we can rapidly insert the E288 beryllium absorber (perhaps temporarily supplemented with polyethylene until additional new beryllium can be obtained if needed) and run the dimuon resonance search as initially proposed.[1]

Beam.

Phase 1: 400 GeV/c protons - 3 x 10^{12}/pulse horizontal spot size: as small as possible (We are insensitive to vertical spot size.)

Phase 2: 160 GeV/c pions 10^{10}/pulse

Tevatron: 1000 GeV/c protons and 400 GeV/c pions at maximum intensity.

Target.

Phase 1: beryllium - 3 in. long
width: as narrow as the beam will allow
(The targets are vertical plates 1 in. high -much larger than the beam vertically. We will also use other solid targets.)

Phase 2: liquid hydrogen/deuterium - 2 m long

Chambers.

Phase 1: PWC 2 and 3 mm spacing
resolution $\delta x \sim 0.6$ mm RMS
(from each station of 3 chambers)

Phase 2: high resolution chambers (see Appendix II)
$\delta x \sim 0.2$ mm RMS

Resolution.

In order to maintain our acceptance[1] without requiring an excessive M3 gap height we have moved M3 somewhat closer to the target. Two momentum measurements are carried out using hit positions at stations 2 and 3 (Fig. 1) in combination with (a) the target position and (b) the hit position in station 1.

		RMS Resolution in %		
		Phase-1	Phase-2	Phase-2 LH_2 Target
Momentum p at 150 GeV/c	$(\delta p/p)_1$	0.7	0.4	6.0
	$(\delta p/p)_2$	2.6	0.9	0.9
Transverse Momentum p_T at 11 GeV/c	$\frac{\delta p_T}{\delta p_T}$	0.24	0.10	0.77
Mass δm at 18 GeV	$\frac{\delta m}{m}$	0.21	0.085	0.60

(We do not include the contributions of inaccuracies associated with the treatment of the magnetic field-nor do we include any contribution from human error, for example in surveying. We include multiple scattering assuming helium fills major drift spaces.)

We stress here that this constitutes a new frontier in resolutions - in some respects this is like a new energy frontier - mini-bumps and narrow resonances have continually appeared to bedazzle particle physics.

Particle Identification.

Phase 1: e/hadron with lead-glass calorimeter (Appendix III)

μ/hadron with hadron calorimeter (Appendix IV)

Phase 2: $\pi/K/p$ (Appendix V)

Trigger.

The dimuon pair trigger depends only on scintillation counters as described in Appendix VIII. For electrons and hadrons, calorimeters are available for triggering if necessary. (Single lepton and hadron triggers may require an on-line processor[2] and single hadrons clearly require prescaling (Fig. 2). In any case extensive use of processors will be made for on-line data reduction and trigger filtering.

MEASUREMENTS TO BE PERFORMED AND TODAY'S SPECIFIC PHYSICS OBJECTIVES

(They will certainly change.)

(1) Single Hadrons.

By comparison of two ~1% momentum measurements and one 10% energy measurement (from the hadron calorimeter) we hope to eliminate background in the high x_T hadron signal out to the kinematic limit. Extrapolating recent measurements at the ISR into the high x_T region, we show in Fig. 2 the π spectrum we would obtain in 2000 hours. We collect reasonable numbers of events out to x_T ~0.9 with either 400 GeV/c or 1000 GeV/c protons incident. (We also show the π spectrum collected from the minimal Tevatron - 800 GeV/c at 10^{11} protons/second, time average.) The extension in p_T available with the Tevatron is substantial (12 to 18 GeV/c) enabling us to get well into the region[3] where the invariant cross section approaches a p_T^{-4} behavior, as expected from dimensional arguments for point scattering.

As indicated earlier, we can learn a great deal about the structure of hadrons simply by measuring the single hadron/lepton ratio as a function of x_T. With pions incident the Drell-Yan process should be even more important at high x_T than indicated in Fig. 2 because of the valence antiquark in the pion.

By identifying single hadrons in the high x_T and high p_T region, clear evidence for the quark structure of hadrons should emerge in the particle ratios as the quark content of the incident

beam is changed.[4] This physics requires $\pi/K/p$ separation, a hydrogen/deuterium target and the super M1 pion beam. Assuming a factor of 300 reduction in intensity with pions (10^{10} per pulse at ~160 GeV/c with 400 GeV/c protons incident) but an increased effectiveness of pions at high x_T of a factor of 10, we should be able to reach $x_T \sim 0.8$ with pions incident. The increase in p_T reached with pions with the coming of the Tevatron (7 to 11 GeV/c) is significant.

(2) Direct Muons.

The double measurement of momentum will hopefully eliminate low momentum background in the direct muon signal out to the kinematic limit. In Fig. 2 we estimate the direct muon rate from our E288 fit to the dimuon continuum.[6] (We integrate over the second muon. See Appendix VII.) We show also 10^{-4} of the pion rate as was observed for $p_T < 5$ GeV/c.[7,8] We see that in our region of p_T, the direct muon/π ratio should rise by a factor of ~10. (The E288 dimuon data[6] go out to m ~15 GeV or p_T ~7 GeV/c. In our extrapolations we have not introduced a cut off for muons at the kinematic limit, $p_T = 13.7$ GeV/c.)

In Fig. 3 we estimate the background due to pion decay in flight (without the beryllium!) It decreases at high p_T for the following reasons:

a) The direct μ/π ratio is expected to increase.

b) The pion decay length increases with its momentum. We include the fact that ~50% of the decays in flight at a given p_T are eliminated by our double momentum measurement. Our microscopic

resolution in p_T avoids smearing toward higher p_T of the decay muons which we do accept. Beyond p_T ~8 GeV/c we should be able to calculate accurately the pion decay background (using simultaneously measured pion distributions) and find the direct muon spectrum by subtraction.

(3) Direct Electrons.

Here we eliminate background with the comparison of two 1% momentum measurements with a 1% energy measurement via the lead-glass calorimeter (at ~150 GeV). The backgrounds due to π^o decay are lower than for $p_T < 5$ GeV/c because of

a) increased ratio direct e/π^o (same as μ/π)

b) increased $p_T \rightarrow$ lower ratio of granddaughter of π^o/π^o

We calculate (see Appendix VII) in Fig. 3 the γ spectrum from π^o decay as well as the $e^{\pm}$ spectrum from Dalitz decay and pair production in the (3 in. beryllium) target. (Here we presume a 5 mm wide target as may be necessary with the pion beam.) The rates for e^- from Compton scattering and from knock-ons are both negligible. In detecting electrons it is important to keep the beam spot and target as thin as possible. With a 5 mm wide, 3 in. long beryllium target we have the pair production background level shown in Fig. 3 and we lose ~10% of the electrons due to energy degradation via bremsstrahlung in the target. If we can run with a 0.2 mm wide target as in E288 these problems drop to negligible levels.

(4) Dimuons.

If we can indeed detect single direct muons cleanly out to the kinematic limit, dimuons will be easy. If we can really attain

~0.1% resolution in mass with 3×10^{12} incident protons per pulse, we will never put in the beryllium. Bump searches without beryllium would then be more sensitive than with beryllium and would allow us to be lower profile users of the accelerator with more physics per incident proton.

(5) Dielectrons.

Again, if we can detect single electrons cleanly, dielectrons should be easy. (We will be able to choose either protons or pions incident.) Due to the large enhancement of the Drell-Yan dileptons produced by a pion beam[9] (~300) it is attractive to run the μ-e universality test with pions. In order to keep the bremsstrahlung loss of electrons as small as possible, it is important to have as small a spot, and as thin a target, as possible. Here the fine optics of the Carey beam are important. We are sensitive only to the spot size in the bend direction.

(6) μe pairs.

The physics interest in μe pairs has been documented.[2] We detect them for free.

(7) Hadron Pairs.

In Fig. 4 we plot our E494 dihadron mass spectrum[10] along with our E288 fit[6] to the dimuon continuum. The two spectra appear to be converging. Theorists are now predicting[11] that with pions incident the dilepton and dihadron spectra will actually cross (within our range). The theorists also point out advantages to studying pairs instead of singles (insensitivity to trigger bias). We will do both.

With hadron pairs, we can extend our earlier data[12] out to the kinematic limits for +/- pairs. Data on x_e scaling and quantum number correlations should be particularly interesting, especially with the availability of the pion beam and a hydrogen target.

(8) A-dependence.

The anomalous A-dependences of both single hadron production and hadron pair production[14] are not understood and are therefore interesting. We have the opportunity to significantly extend the previous measurements.

REFERENCES

[1]Proposal 605.

[2]Letter of June 12, 1978 to the PAC.

[3]A. G. Clark et al., (CERN-Saclay-Zurich group), CERN preprint (unnumbered). At $\sqrt{s}$ = 27.4 GeV (400 GeV/c incident momentum) this fit agrees within a factor of 3 with the CCOR fits (as presented by R. Cool in Tokyo) and the Chicago-Princeton fits (D. Antreasyan et al., EFI 78-29) for $5 < p_T < 12$ GeV/c.

[4]Proposal 586.

[5]G. Donaldson et al., PRL 36, 1110 (1976).

[6]D. Kaplan et al., PRL 40, 435 (1978).

[7]J. P. Boymond et al., PRL 33, 112 (1974).

[8]J. A. Appel et al., PRL 33, 722 (1974).

[9]K. J. Anderson, Session A10-(4) at Tokyo.

[10]R. D. Kephart et al., PRL 39, 1440 (1977).

[11]Krawczyk and Ochs, Max Planck Institute preprint, July 1978.

[12]R. J. Fisk et al., PRL 40, 984 (1978).

[13]L. Kluberg et al., PRL 38, 670 (1977).

[14]R. McCarthy et al., PRL 40, 213 (1978).

FIGURE 1

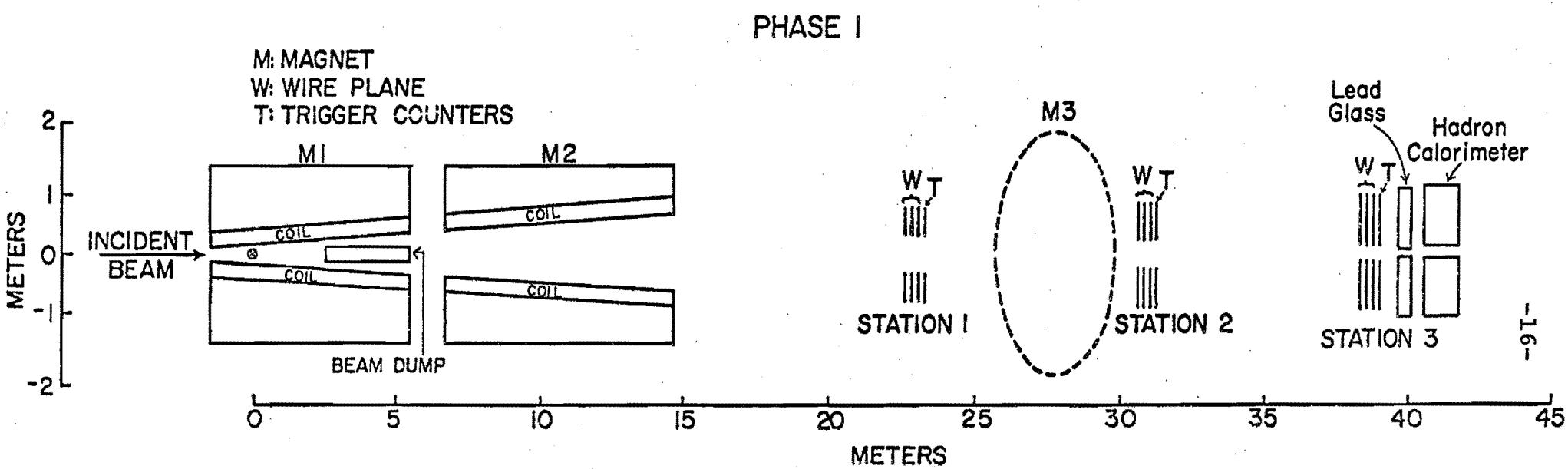
PHASE I
M: MAGNET
W: WIRE PLANE
T: TRIGGER COUNTERS
M1
M2
M3
COIL
INCIDENT BEAM
BEAM DUMP
W
T
STATION 1
STATION 2
STATION 3
Lead Glass
Hadron Calorimeter
METERS
2
1
0
-1
-2
0
5
10
15
20
25
30
35
40
45
METERS

FIGURE 2

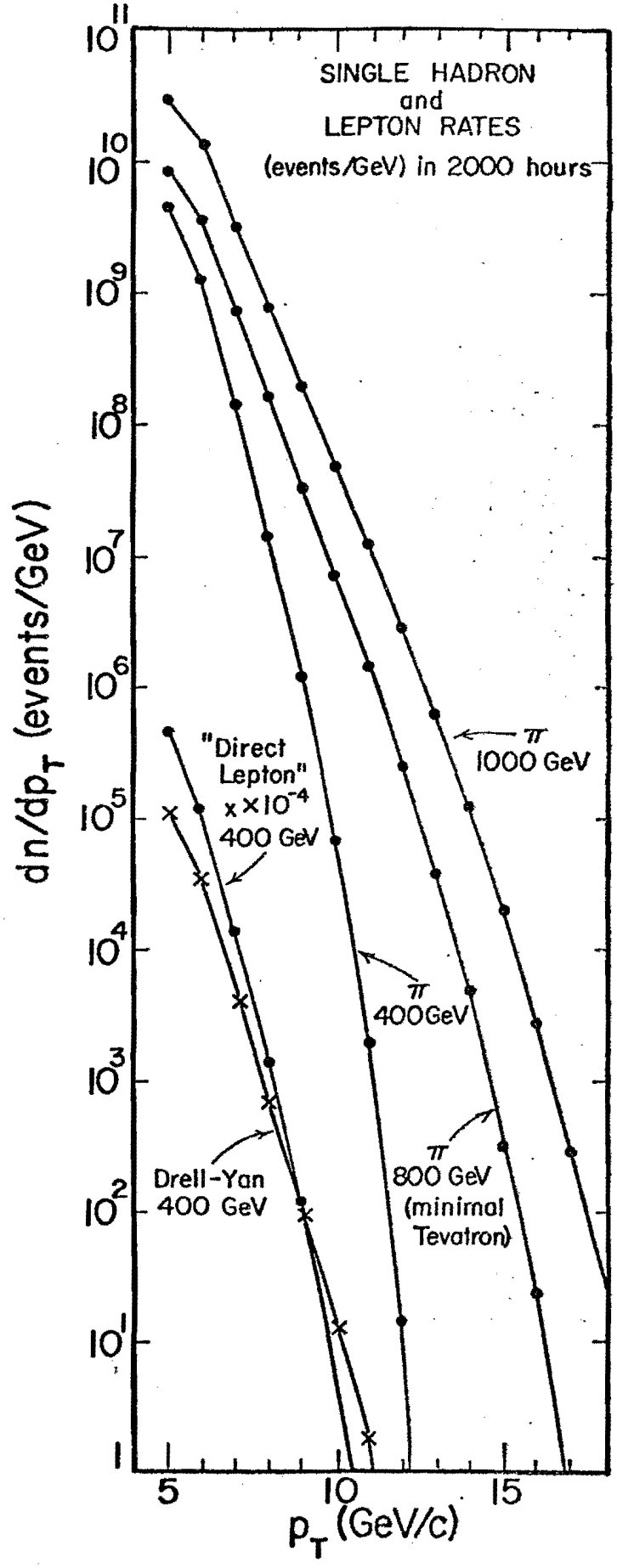
SINGLE HADRON
and
LEPTON RATES
(events/GeV) in 2000 hours
dn/dp_T (events/GeV)
p_T (GeV/c)
"Direct Lepton" x×10^-4 400 GeV
π 1000 GeV
π 400GeV
π 800 GeV (minimal Tevatron)
Drell-Yan 400 GeV

FIGURE 3

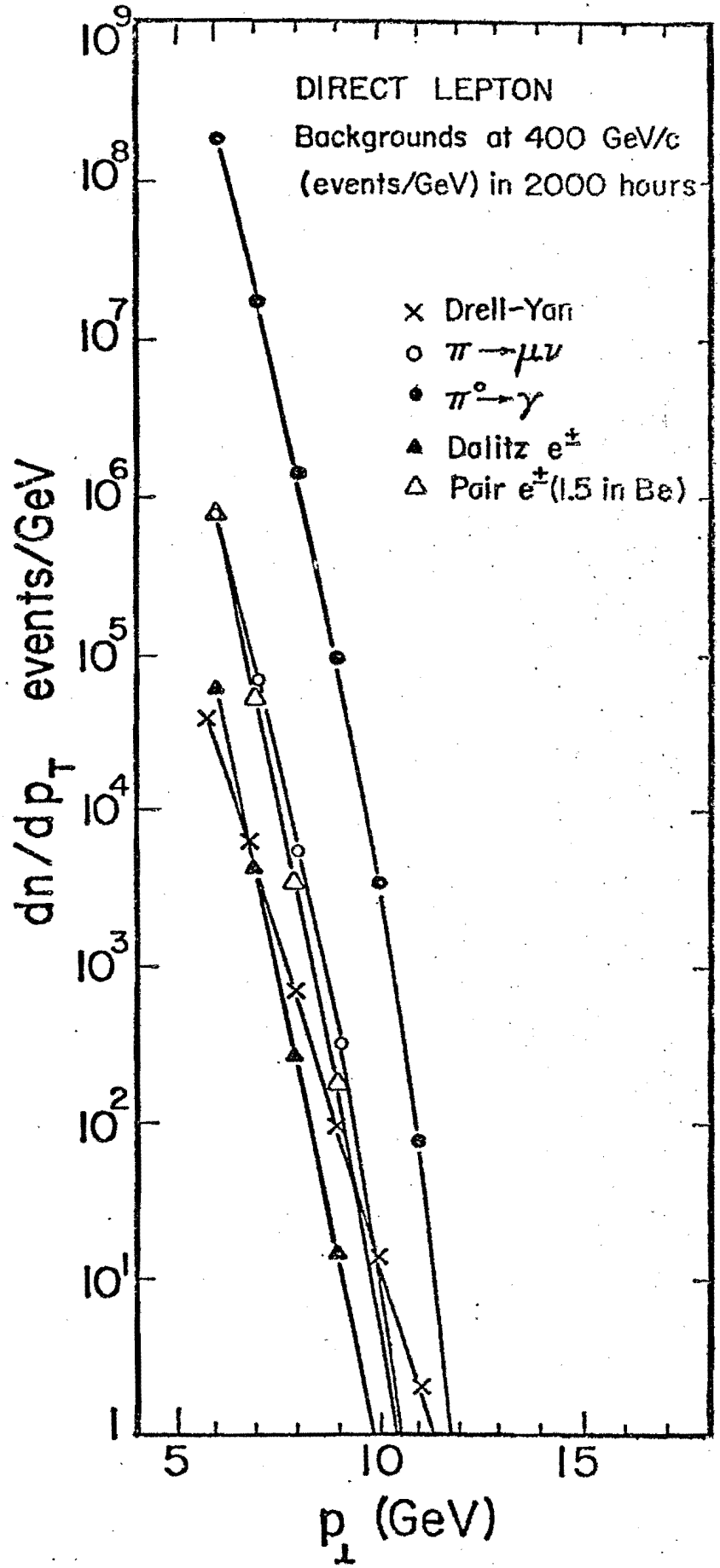
DIRECT LEPTON
Backgrounds at 400 GeV/c
(events/GeV) in 2000 hours
× Drell-Yan
○ $\pi \to \mu\nu$
● $\pi^0 \to \gamma$
▲ Dalitz $e^\pm$
△ Pair $e^\pm$(1.5 in Be)
dn/dp_T events/GeV
10^9
10^8
10^7
10^6
10^5
10^4
10^3
10^2
10^1
1
5
10
15
$p_\perp$ (GeV)

FIGURE 4

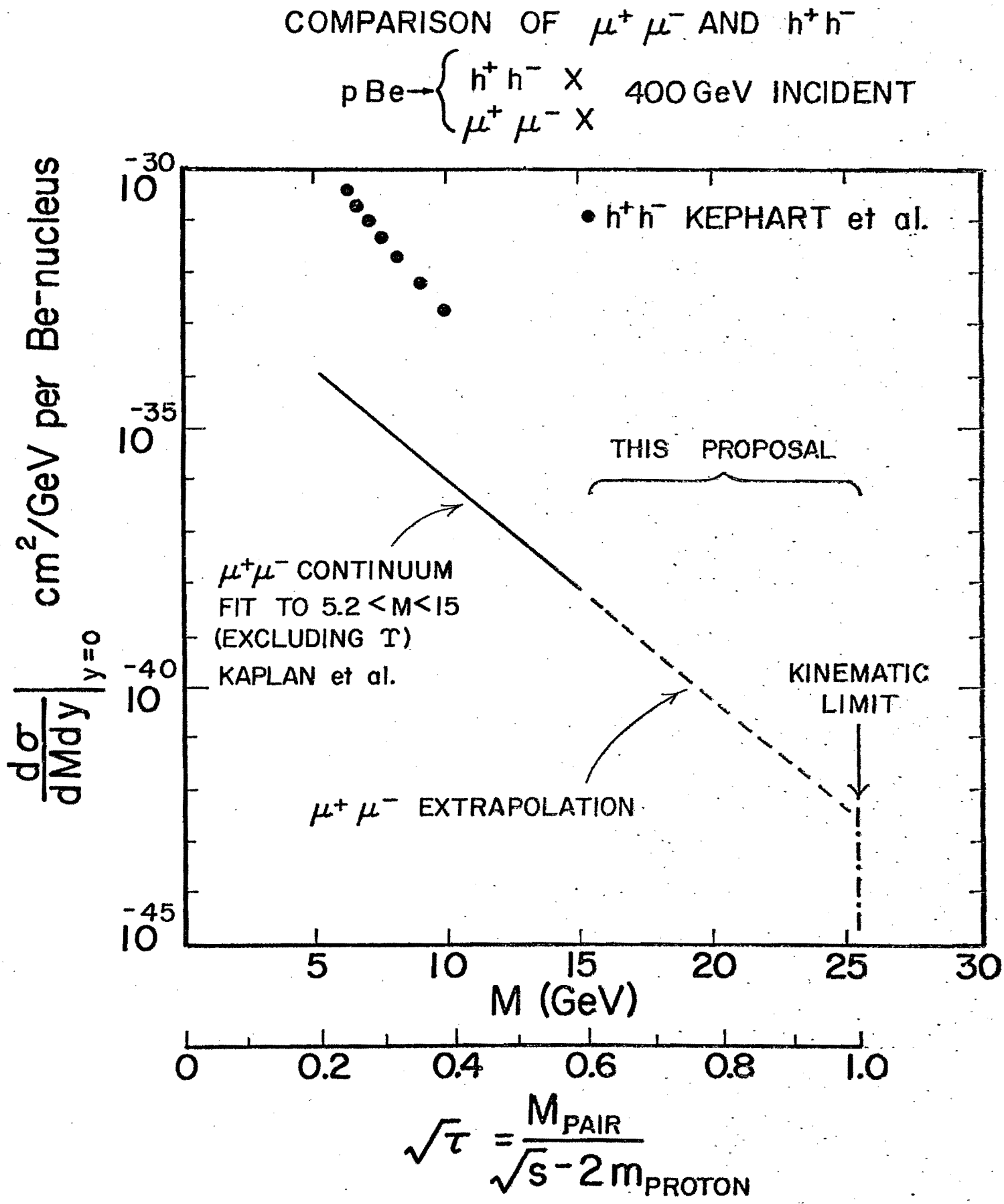
COMPARISON OF $\mu^+\mu^-$ AND h^+h^-
p Be → { h^+h^- X, $\mu^+\mu^-$ X } 400 GeV INCIDENT
$\frac{d\sigma}{dMdy}\Big|_{y=0}$ cm²/GeV per Be-nucleus
10^{-30}
10^{-35}
10^{-40}
10^{-45}
• h^+h^- KEPHART et al.
THIS PROPOSAL
$\mu^+\mu^-$ CONTINUUM
FIT TO 5.2 < M < 15
(EXCLUDING Υ)
KAPLAN et al.
KINEMATIC LIMIT
$\mu^+\mu^-$ EXTRAPOLATION
5
10
15
20
25
30
M (GeV)
0
0.2
0.4
0.6
0.8
1.0
$\sqrt{\tau} = \frac{M_{PAIR}}{\sqrt{s} - 2m_{PROTON}}$

APPENDIX I: NEVIS CYCLOTRON

We can assess the difficulties involved in moving the Nevis cyclotron to Fermilab by considering experience with the Chicago cyclotron. The magnets are quite similar. We propose to use only the basic yoke, without the field shaping pole tips (which are radioactive anyway).

Basic yoke:	height	21 ft.
	width	33 ft.
	depth	14.2 ft.
Pole (circular):	diameter	13.5 ft.
Gap height:		5.0 ft.

Coils: We propose to use the superconducting coils which have been wound for the Chicago cyclotron at Fermilab. The Nevis coils are very old-fashioned (oil-cooled).

Power supply: The Nevis supply is available, but may be inconvenient to use.

Pieces to be moved:

#	size	weight (tons)
20	33' x 5.25' x 17"	60.3
10	10.5' x 5.25' x 34"	38.3
4	13.5' diam - 16 3/8" high	48.0
	Total	1781 tons

Difficulties:

(1) Vacuum chamber, dee etc. must be removed. The work is difficult and the area is radioactive.

(2) The cyclotron is welded together at several points.

Both problems were encountered with the Chicago cyclotron.

Transportation:

(1) Nevis has a 60 ton crane. This crane can disassemble the cyclotron and put the pieces on a truck.

(2) Must rent a crane to put the pieces on railroad cars (or barge) in New York.

(3) Must rent a crane to load trucks at Fermilab rail and then unload trucks and assemble the cyclotron.

APPENDIX II: CHAMBERS

Phase 1. Our phase 1 system is the E288 system which presently exists - multiwire proportional chambers with 2 and 3mm spacing.

Resolution: $\delta x \approx 0.6$ mm per station

Time Resolution: $\delta t \approx 70$ nsec (3 buckets)

Phase 2. Charpak and Sauli are developing a new type of detector[1] for use in this experiment:

Resolution: $\delta x \approx 0.2$ mm

Time resolution: $\delta t \approx 20$ nsec (1 bucket)

In addition to the greatly improved resolution in space and time, these chambers have a built in time delay (allowing time for logic decisions) and a two dimensional readout. Applications in imaging Čerenkov counters are particularly interesting (Appendix V). We request Fermilab support (e.g. test beam time) in order to develop this new detector.

---

[1] G. Charpak and F. Sauli, The Multistep Avalanche Chamber: A New High-Rate, High-Accuracy Gaseous Detector, CERN preprint (unnumbered), submitted to Physics Letters B

APPENDIX III: LEAD-GLASS CALORIMETER

If we allow 15m for a hadron species identification system (Fig. 1) the lead-glass calorimeters are placed 45m from the target. At this position an area of approximately $1.3 \times 2.2 = 2.9\ m^2$ must be covered with lead-glass for each arm. Each arm of the E288 lead-glass calorimeter[1] covers $1.7\ m^2$ with 25.8 radiation lengths of lead-glass. Consequently we own $\sim 2/3$ of the required lead-glass. The expected energy resolution[1] for electrons of energy E(GeV) is

$$\frac{\delta E(\mathrm{RMS})}{E} = 0.0064 + \frac{0.043}{\sqrt{E}}$$

[1] D.C. Hom, Thesis, Columbia University, Nevis 222, Nevis Laboratories (1977)

APPENDIX IV: HADRON CALORIMETERS

We need two hadron calorimeters, each 1.5 x 2.4 m^2. We have estimated the cost of two such 6.5 interaction length calorimeters, each consisting of 40 one inch steel plates separated by 1/4 inch slabs of acrylic scintillator. The scintillator is segmented into 8 inch strips horizontally. The energy signals from both top and bottom of each strip are read out by 1/4 inch thick wave shifter bars into 20 fast phototubes for each calorimeter.

expected resolution[1]: $\frac{\delta E(\mathrm{RMS})}{E} \simeq 0.1$

estimated cost: $ 80K

[1] F.J. Sciulli, "Photon-Collecting Hadron Calorimeters", P.114 in Proceedings of the Calorimeter Workshop, Fermilab, May 1975.

APPENDIX V: HADRON SPECIES IDENTIFICATION

We wish to identify hadrons in the momentum range 100-300 GeV/c. (With the Tevatron the desired range extends to 500 GeV/c.) At present there is no proven method to perform $\pi/K/p$ separation in this momentum range in a large aperture detector, so we will attempt to develop the appropriate technology.

Imaging Cerenkov Counter

At the present time we feel the most fruitful approach is to attempt to build a wide aperture imaging Cerenkov counter. Much work[1-5] has been done in this area recently. Our plan of attack is to use the multistep avalanche chamber[6] of Charpak and Sauli as an ultraviolet photoionization detector. Such a chamber has the following advantages:

1. Multistep amplification allows stable operation at gains large enough to detect single photons.[6] Instabilities appear to depend only on the gain/step. This overcomes a difficulty observed in earlier work.[1]
2. Good spatial resolution: $\delta x \sim 0.2$ mm rms.
3. Good time resolution: $\delta t \sim 20$ nsec. This chamber has essentially no dead time.
4. Multidimensional readout: The electron swarms resulting from amplification may be drifted across as many gaps as desired. Each gap can contain a wire plane reading out a projection of the Cerenkov ring image.

An unsolved difficulty with this approach is reconstruction of the ring image in two dimensions given the hit location projections. Our hopes are that it may be possible to:

a) associate hit projections by measuring pulse heights of individual avalanches (if they have a large spread),

or b) use the projections themselves to measure the ring radius.

The pattern recognition problem is unsolved but may be considerably simplified by looking for a pattern appropriate to π, K or p about a track with a known momentum. For high efficiency, we require at least an average of 6 photons detected per incident track.

The number of photons emitted per cm of particle path length is given by[1]

$$\left(\frac{dn}{dx}\right)_{emitted} = N_o^e \sin^2\theta_c$$

where $N_o^e = 370\ (E_2-E_1)$ photons/cm, θ_c = Cerenkov emission angle, and E_2-E_1 = range of photons detected (eV).

In existing photoionization detectors[1] E_1 is given by the threshold for ionization of the photoionizing gas and E_2 is the threshold for absorption in the detector window. Benzene[1,5] (E_1 = 9.25 eV) has been used successfully as the photoionizing gas in a 1% mixture with Argon. Triethylamine (E_1 = 7.5 eV) has also been used successfully[6] and is particularly promising because of its low threshold. Windows of LiF (E_2 = 11.8)[2] and Mg F_2 (E_2 = 11.2 eV)[5] have both been used but because LiF is hygroscopic,[5] we take $E_2 - E_1$ = 3.7 eV as appropriate for triethylamine

and Mg F_2. In this case

$$N_o^e \sim 1370 .$$

An attraction of the photoionization process is that quantum efficiencies exceeding 60% have been attained.[1] Therefore, we presume here that 35% of the emitted photons are actually detected (after one reflection from a mirror and transmission through the Mg F_2 window). Then

$$\left(\frac{dn}{dx}\right)_{detected} = N_o \sin^2\theta_c$$

with $N_o \simeq 480$ photons/cm.

Helium is the best Cerenkov radiator in the high momentum region because it has

1. the highest Cerenkov threshold at atmospheric pressure

$$\gamma_t \equiv \left.\frac{1}{\sqrt{1 - (V/c)^2}}\right|_{\substack{at \\ threshold}} = \frac{1}{\sqrt{2\ (n-1)}} = 113$$

(with $(n-1) = 39.4 \times 10^{-6}$ for 9.35 eV photons[7]).

2. very little dispersion[7]

$$\Delta n \equiv n\ (11.2\ eV) - n\ (7.5\ eV) = 4.9 \times 10^{-6}.$$

For a particle above threshold the Cerenkov angle is given by

$$\sin\theta_c = \frac{1}{\gamma_t} \left[\frac{1 - (\gamma_t/\gamma)^2}{1 - (1/\gamma)^2}\right]^{1/2} .$$

The numbers of photons detected from a length L = 15 m of He for π, K, p are plotted as a function of momentum in Fig. A VII.1 and the corresponding Cerenkov ring radii r are plotted in Fig. A VII.2 assuming a mirror with focal length f = 3 m ($r = f\,\theta_c$). We see that the number of photons detected is quite large: typically 50. This large number encourages us to believe that the ring radii could indeed be determined from the projections alone. Then the multidimensional readout could be used to resolve ambiguities among whole ring patterns rather than among individual hits. This approach seems quite promising. If we presume then an rms resolution in ring radius $\delta r \simeq 0.2$ mm, considering <u>only</u> a single measurement of r, we see that this counter could perform the π/K separation from 16 to 300 GeV/c and the K/p separation from 60 to 600 GeV/c. It would thus be quite adequate for our pre-Tevatron running.

We must, however, consider the potentially devastating effects of dispersion of the index of refraction n as well as the improvement due to the multiple measurements possible on a single event. It can be shown[1] that the resolution in mass of the particle to be identified is given by

$$\frac{\delta m}{m} = \frac{\delta\gamma}{\gamma} \simeq \frac{\gamma^2\ \delta\theta_c}{\sqrt{N_o L}} \quad \text{at fixed momentum,}$$

where we treat each photon as providing an independent measurement of θ_c with rms deviation

$$\delta\theta_c = \left[\left(\frac{\delta r}{f}\right)^2 + \left(\frac{\delta n}{n \tan\theta_c}\right)^2\right]^{1/2} \quad \text{with } \delta n \simeq \Delta n/\sqrt{12} \text{ for a single photon}$$

$$= \left[(6.7 \times 10^{-5})^2 + (1.63 \times 10^{-4})^2\right]^{1/2}$$

$$= 1.76 \times 10^{-4}$$

so $$\frac{\delta m}{m} = \gamma^2 \times 2.07 \times 10^{-7}$$

We find the maximum momentum P_{max} for π/K separation by requiring

$$\delta m_\pi + \delta m_K = (m_K - m_\pi) = \left(\frac{1}{m_K} + \frac{1}{m_\pi}\right) P_{max}^2 \times 2.07 \times 10^{-7}$$

$$P_{max} = \left[\left(\frac{m_K - m_\pi}{m_K + m_\pi}\right) m_K m_\pi / 2.07 \times 10^{-7}\right]^{1/2}$$

$$P_{max}^{\pi/K} = 430 \text{ GeV/c} .$$

We find in a similar fashion

$$P_{max}^{K/p} = 880 \text{ GeV/c} .$$

However, as indicated above, it is probably a bit too optimistic to consider each photon as providing an independent measurement of δr.

Conclusion

An imaging Cerenkov counter containing 15 m of helium at atmospheric pressure seems capable of providing $\pi/K/p$ separation up to momenta of ~400 GeV/c. Dispersion is a major source of uncertainty. In order to reach even higher momenta at atmospheric pressure it is desirable to find a gas with an even lower photoionization threshold than 7.5 eV. The additional photons accepted would have relatively little dispersion.

A 15 m Cerenkov counter would be placed between chamber stations 2 and 3. (See Fig. 1 of the Addendum.) Station 3 (and the calorimeters) would be moved back to ~46 m from the target.

References from Appendix V

[1]J. Seguinot and T. Ypsilantis, Nucl. Instrum. Methods 142, 377 (1977).

[2]V. Ashford et al., "Cerenkov Counters at ISABELLE", Proceedings of the ISABELLE Summer Study (1978). We thank V. Ashford for providing us with a preliminary copy of this very useful document.

[3]S. Durkin et al., "Preliminary Results on Tests of a Cerenkov Ring Imaging Device Employing a Photoionizing PWC", Proceedings of the ISABELLE Summer Study (1978).

[4]J. Chapman et al., "Operation of a Cerenkov Counter with an Ultraviolet Photoionization Detector", University of Michigan preprint, UM HE 78-23.

[5]R. S. Gilmore et al., "An Observation on the Spatial Distribution of Vacuum UV Photons Generated by Cerenkov Radiation", Rutherford Lab preprint (unnumbered).

[6]G. Charpak and F. Sauli, The Multistep Avalanche Chamber: A New High-Rate, High-Accuracy Gaseous Detector, CERN preprint (unnumbered) 9/12/78, submitted to Physics Letters B.

[7]M. C. E. Huber and G. Tondello, "Refractive Index of He in the Region 920-1910 Å", Journal of the Optical Society of America 64, 390 (1974). It is interesting to note that these authors used a grating spectrograph with no windows.

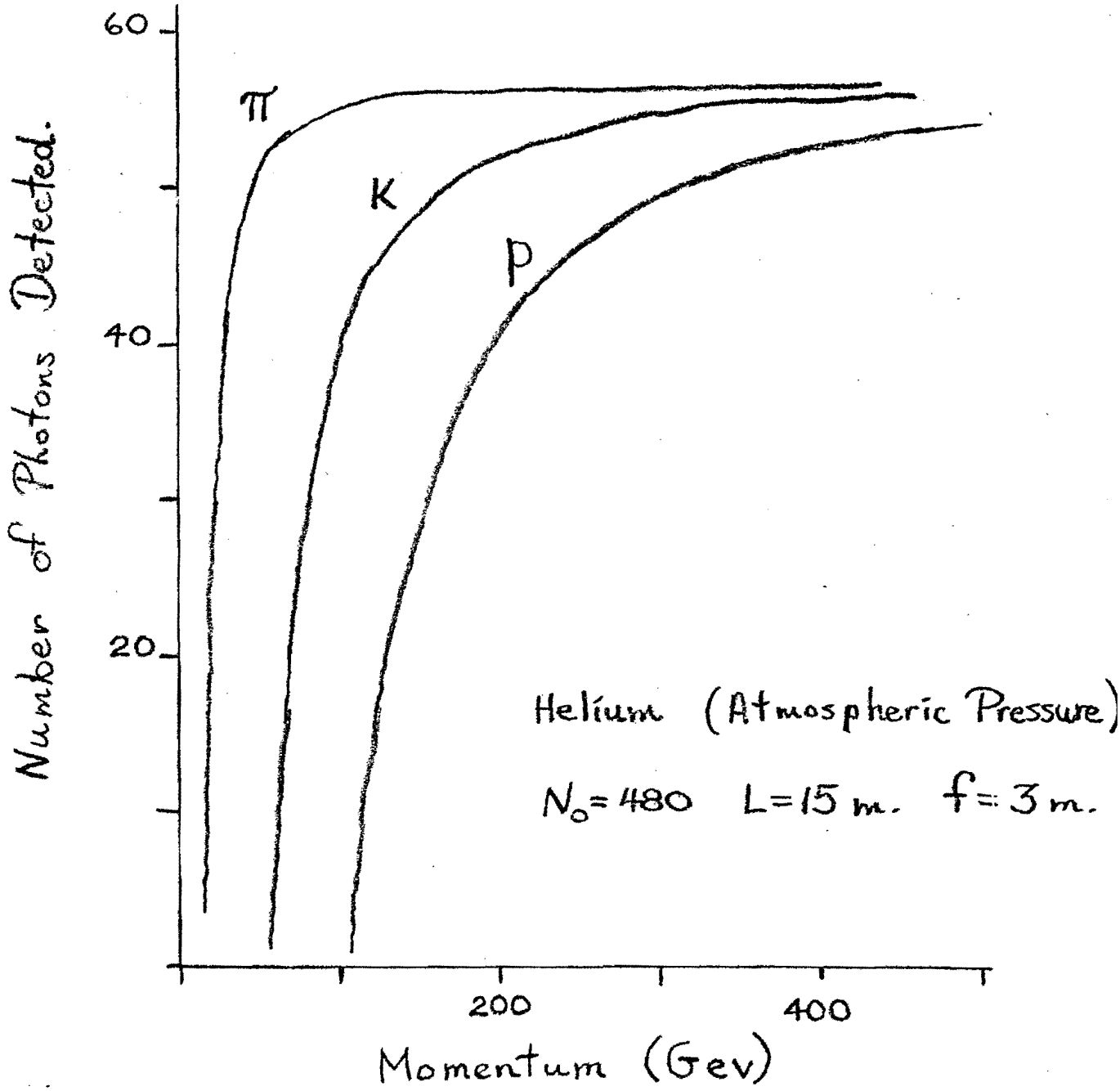
60
40
20
Number of Photons Detected.
π
K
p
Helium (Atmospheric Pressure)
N_o = 480 L = 15 m. f = 3 m.
200
400
Momentum (Gev)

Fig. A VII.1

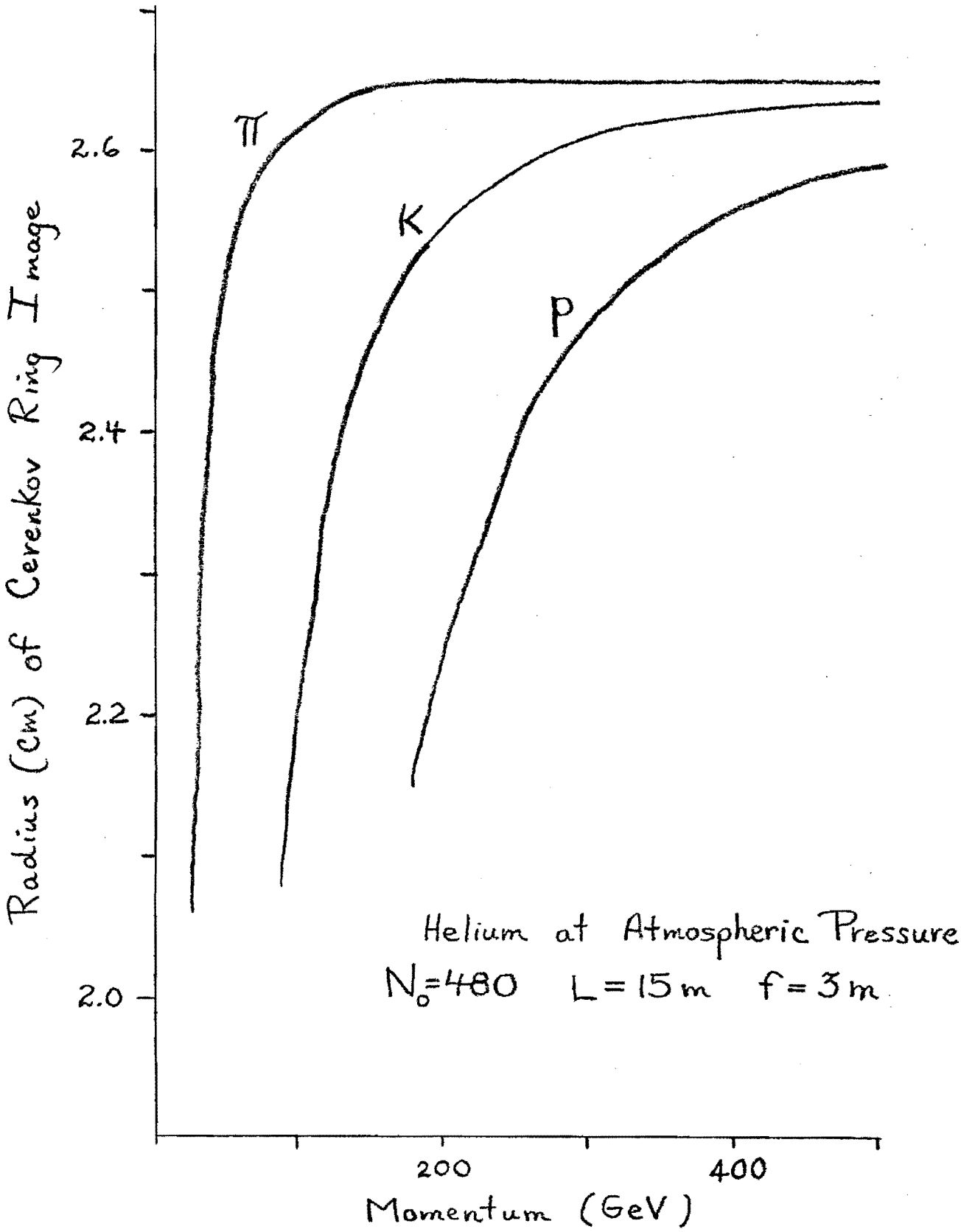
Radius (cm) of Cerenkov Ring Image
2.6
2.4
2.2
2.0
π
K
P
Helium at Atmospheric Pressure
N_o=480 L=15 m f=3 m
200
400
Momentum (GeV)

Fig. A VII.2

APPENDIX VI: RADIATION

Since we plan to run at high intensity in the Meson Lab, an above-ground laboratory, radiation is a potentially serious problem. The main difficulty comes from muons generated by π decay in flight in the hadronic cascade in the dump. The cleanest method of attack is to cause the pions to interact before they can decay. So in order to alleviate the muon problem, both for our experiment and for personnel, we ask that our dump contain a tungsten core. We envision the dump as a solid block of copper (~2 tons) with holes drilled for water cooling and a hole drilled from the back to insert the tungsten plug. After the plug is inserted, the resulting hole should be welded shut. Then as long as the cooling water is capable of removing the 200 kilowatts deposited by the beam before the copper block cracks, the dump should survive. We would like to work with the laboratory in exploring the feasibility of such a dump.

During the high intensity tests in the Meson Lab for E439 it was found[1] that the muon radiation problem could be handled up to our requested incident intensity of 3×10^{12}. Our geometry should be cleaner than that of E439 for the following reasons:

1) Our tungsten dump should allow approximately a factor of 2 fewer muons to escape,
2) Our magnets give a factor of 3 larger p_T kick to emerging muons. Hence the problem is spread over a larger area

providing lower levels of radiation at our detectors which are smaller than those of E439 in terms of solid angle from the target.

If necessary, we would be willing to sweep vertically as did E439. However, we would prefer to remain in a horizontal plane, pitching the incident beam and the experiment downhill by ≈10 mrad so that the muons head underground a few hundred meters north of the Meson Detector Building.

We are in the process of calculating the muon distributions by Monte Carlo, both with the proton beam and with the pion beam in phase 2.

Reference

[1] T. E. Toohig, TM-815, Fermilab, September 22, 1978.

APPENDIX VII: DETAILS OF CALCULATIONS

1. Direct Muons

For the purpose of this calculation we assume that Drell-Yan muons are produced isotropically in the dimuon rest frame. Then if m, Y and $\vec{P}_T$ are the mass, rapidity and vector transverse momentum of the dimuon, the 6 fold two muon differential cross section is given (exactly) by

$$E_1 E_2 \frac{d^6\sigma}{d^3P_1 d^3P_2} = \frac{1}{2\pi\ p_{CM}} \frac{d^4\sigma}{dmdY\ d^2P_T}$$

where $p_{CM} \equiv \left|\vec{P}_1 - \vec{P}_2\right|_{\substack{\text{center of}\\ \text{momentum}}} \simeq m$.

Therefore

$$E_1 \left.\frac{d^3\sigma}{d^3P_1}\right|_{\substack{\text{single muon}\\ \text{from a pair}}} = \int_{\text{all } \vec{P}_2} \frac{dy_2 d\phi_2 P_{T2} dP_{T2}}{2\pi\ m} \frac{d^4\sigma}{dmdY\ d^2P_T}$$

Since all previous data on lepton and hadron production at high P_T has been taken at 90° in the center of momentum frame (CM), we evaluate all cross sections at 90° CM. In accord with the E288 continuum fit (Addendum Ref. 6) we take

$$\frac{d^4\sigma}{dmdY\ d^2P_T} = C\ e^{-bm}\ K\left[1 + (P_T/2.8)^2\right]^{-6}$$

with $C = 2.60 \times 10^{-33}\ cm^2/GeV$

$b = 0.986\ GeV^{-1}$

$K = 0.203\ GeV^{-2}$.

If we hold particle 1 fixed at 90° CM the range in ϕ_2 is limited by the fact that the muons have a virtual photon parent with $\langle P_T \rangle \sim 1.2$ GeV/c. We simply take flat dependences in ϕ_2 and y_2 over the limited ranges

$$\Delta\phi_2 = \frac{2 \times 1.2 \text{ GeV/c}}{P_{T2}} \qquad \Delta y_2 = 1 \ .$$

Thus we are limited to reasonably symmetric pairs so that we may make the approximations

$$m \simeq P_{T1} + P_{T2} \qquad P_T \simeq \left| P_{T1} - P_{T2} \right| \ .$$

Thus

$$E_1 \left.\frac{d^3\sigma}{d^3P_1}\right|_{\substack{90^{\circ} \\ \text{in CM}}} \sim \frac{2.4\Delta y_2}{2\pi} CK \int_0^{\sqrt{s}/2} \frac{dP_{T2}}{P_{T1}+P_{T2}} e^{-b(P_{T1}+P_{T2})} \left[1+\left[\frac{(P_{T1}+P_{T2})}{2.8}\right]^2\right]^{-6} .$$

We have evaluated this integral by numerical integration for each P_{T1}. The accepted single muon spectrum is then given by

$$\frac{dn}{dP_T} = L \ A \ P_T \left(E_1 \frac{d^3\sigma}{d^3P_1}\right)$$

where

$L = 1.5 \times 10^{43}$ is our integrated luminosity (2000 hours)

$A \simeq 0.9$ steradians (essentially our CM solid angle).

The results are plotted in Fig. 2. As expected, the spectrum is closely proportional to e^{-2P_T}. (Remember that $m \simeq 2\ P_T$.)

2. Pion Decay in Flight

The pion spectrum was taken from recent ISR data (Addendum Ref. 3). Since the maximum transverse momentum delivered to a muon in pion decay is 30 MeV/c, we assume the muon keeps the same direction as the pion. Then

$$\frac{dn_\mu}{dp_T} = \frac{\theta\ m_\pi z}{(1-f)c\tau} \int_{P_T}^{p_{T/f}\ \text{or}\ \sqrt{s}/2} \frac{dn_\pi}{dP'_T}\ \frac{dP'_T}{P'^2_T}$$

where θ = production angle $\simeq 0.06$

z = available decay length

$c\tau$ = pion decay length = 7.8 m

$f = (m_\mu/m_\pi)^2 = 0.57$

This integral was evaluated by numerical integration to produce the results shown in Fig. 2. The background in μ^+ will be about a factor of 2 higher than shown due to the decay of K^+.

3. e^+e^- Pairs

The rate for γ's from π^o is given by

$$\frac{dn_\gamma}{dP_T} = 2\int_{P_T}^{\sqrt{s}/2} \frac{dn_\pi}{dP'_T}\ \frac{dP'_T}{P'_T} \simeq 4.05 \times 10^{15}\ \frac{(1-X_T)^{9.6}}{P_T^{7.64}}$$

where the integrals were performed by numerical integration. The quoted form fits the results of the integrations to an accuracy of 30%. Then the rate for electrons or positrons from Dalitz decay is given by

$$\left(\frac{dn_e}{dP_T}\right)_{\text{Dalitz}} = P_D \int_{P_T}^{\sqrt{s}/2} \frac{dn_\gamma}{dP_T'} \frac{dP_T'}{P_T'}$$

where $P_D = 0.0115/2 = 5.75 \times 10^{-3}$. The rate for pair production in 1.5 in. of beryllium is

$$\left(\frac{dn_e}{dP_T}\right)_{\substack{\text{pair}\\ \text{production}}} = P_P \int_{P_T}^{\sqrt{s}/2} \frac{dn_\gamma}{dP_T'} \frac{dP_T'}{P_T'}$$

$$P_P = 6.97 \times 10^{-2} .$$

APPENDIX VIII: TRIGGER

The mass-focusing feature and the basic two-particle trigger of the proposed apparatus are demonstrated in Fig. AVIII.1. For a two-particle trigger, we require a track on each side of the center line and a proper combination of T1, T2, and T3 hodoscope elements. In part (a) a high mass event with M ≈ 20 GeV is shown which properly satisfies the trigger requirements. An event with intermediate mass (M ≈ 14 GeV) is shown in part (b). Here, the positive and negative particle trajectories have crossed over the center line, and, for this example, both have missed the hodoscope at station 1. This demonstrates the utility of the gaps along the center line: trajectories from particles of intermediate mass fall in one or more gaps and thus do not provide a proper trigger. In part (c) a low mass (≈10 GeV) particle produces trajectories which again cross over the center line, but still strike all three hodoscope stations. However, these low mass events can be eliminated by requiring an appropriate combination of T1, T2 and T3 elements.

In addition to the horizontal segmentation of the trigger counters/hodoscope shown in Fig. AVIII.1, each counter will be split vertically into an upper and lower half. Requiring the tracks to strike the upper (or lower) half on each side of the center line will eliminate some spurious tracks which do not originate in the target. This vertical (non-bend) angle

FIGURE AVIII.1

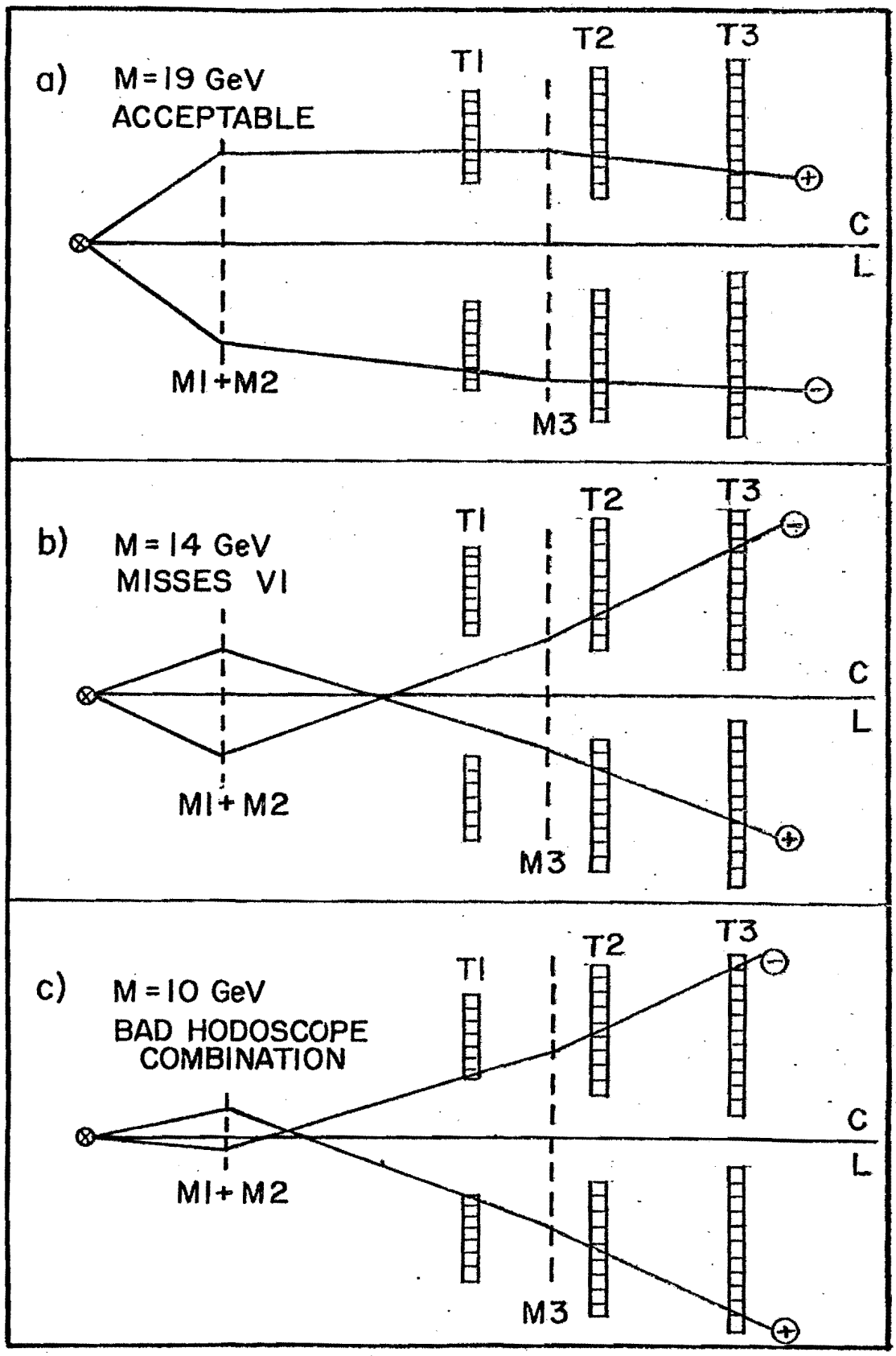

determination can be substantially improved, if necessary, with an additional, more finely segmented vertical hodoscope.

The trigger efficiency as a function of dimuon mass of this proposed arrangement has been investigated with a Monte Carlo program and is demonstrated in Figs. AVIII.2 and 3. (For these purposes, the program generated dimuon events originating in the target, with a flat distribution in mass rather than the steeply decreasing spectrum measured by E288.) In Fig. AVIII.2 the number of dimuon events is displayed which can traverse a pseudo-apparatus with no gaps along the center line, and no trigger. Here, we see that dimuons with $6 \leq M \leq 26$ GeV can produce two muon trajectories, each of which can pass through the aperture of such a pseudo-apparatus. Fig. AVIII.3 demonstrates the effects of the gaps and the hodoscope trigger on events in this aperture. In part (a) we show the fraction of events in this aperture which are simply required to have a hit on each side of the center line at the three trigger counter planes. The severe suppression of intermediate mass dimuons by this simple minimal trigger is evident, as is the complete transparency of this minimal trigger for $M \geq 19$ GeV, as well as $M \leq 8$ GeV. In part (b) we show the fraction of events in the aperture which satisfy this minimal trigger when there are gaps along the center line between the two sides of the apparatus. Here, the combination of the gaps with the minimal trigger completely eliminates dimuons of intermediate mass ($12 \leq M \leq 16$ GeV). This clear separation of high and low mass by this minimal trigger with gaps results in a clean separation of the angular distributions

FIGURE AVIII.2

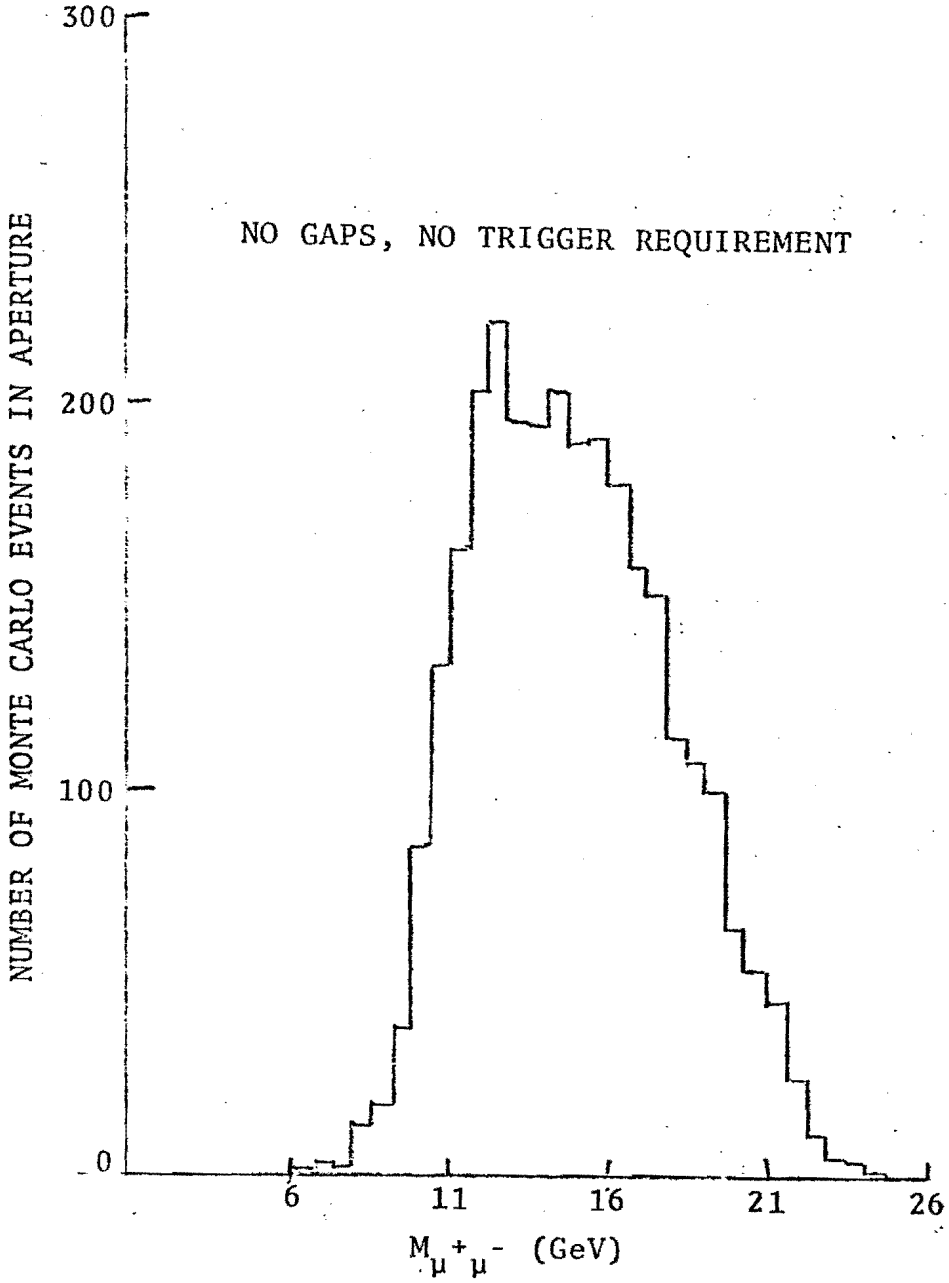

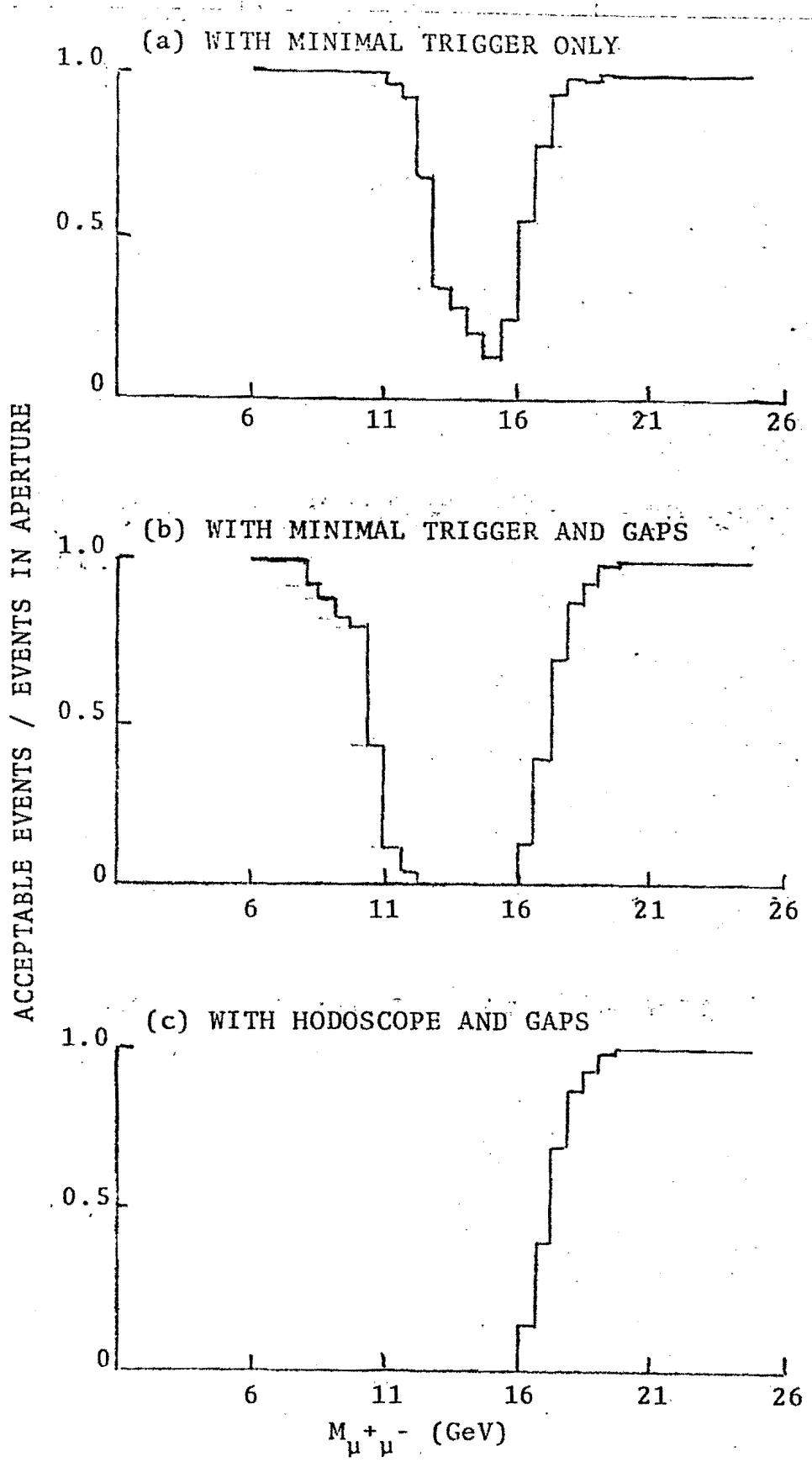
(a) WITH MINIMAL TRIGGER ONLY
(b) WITH MINIMAL TRIGGER AND GAPS
(c) WITH HODOSCOPE AND GAPS
ACCEPTABLE EVENTS / EVENTS IN APERTURE
1.0
0.5
0
6
11
16
21
26
$M_{\mu^+\mu^-}$ (GeV)

of the two muons from the two mass ranges. This clean separation of angles in turn allows the hodoscope, as described in the previous paragraphs, to eliminate the low mass events without disturbing the high mass events. The final design trigger efficiency as a function of parent mass is shown in Fig. AVIII.3c. We stress that no dimuon with $M \geq 20$ GeV, which can pass through the aperture, is effected by the gaps or the hodoscope, and that no dimuon with $M \leq 15$ GeV alone can properly satisfy the trigger requirements.

APPENDIX IX: COMPETITION

Dileptons

Mainly from PETRA and PEP.

(See Addendum Ref. 2.). In the channel $\pi N \rightarrow \mu^+\mu^-$ the Chicago-Princeton group is expected to make a good measurement on the continuum. Their statistics will be comparable to ours but our resolution is much better.

Single Leptons

We know of no other experiment which can approach our systematic control at high p_T. This is very important for single leptons.

Single Hadrons

If we run at 3×10^{12} protons/pulse we have a luminosity of 2×10^{36} cm^{-2} sec^{-1} into a CM solid angle of 2 steradians. A typical ISR experiment might have a solid angle 3 times larger but a luminosity lower by a factor of 2×10^4. With our low s we are uniquely suited to probe the kinematic limit at high X_T. We have the advantage over the ISR of being able to study interactions with pions incident.

Compared to the Chicago-Princeton π beam experiment we have a solid angle advantage of a factor of $\sim 5 \times 10^3$. They, however, have a working Cerenkov system.

Dihadrons

With our high luminosity and low s, we are uniquely suited to study correlations near the kinematic limit. The availability of a π beam is particularly important.

APPENDIX X: IMPACT OF THE TEVATRON

Since we probe the kinematic limits, the increase in s available with the Tevatron provides dramatic increases in the ranges we cover in mass and p_T. We may cross at least two important thresholds within this increased range.

1. Dilepton Resonances

The Tevatron (minimal Tevatron) will allow us to extend our dilepton mass range from 20 GeV to 29 GeV (25 GeV). Many physicists' favorite numerology places toponium within this range.

2. Constituent Scattering

There is evidence from the ISR (Addendum Ref. 3) that single hadron production has a P_T dependence (at constant X_T) approaching a P_T^{-4} behavior for $P_T > 9$ GeV/c. If the onset of such behavior were complete, it would have the same significance for constituents in the proton as the q^{-4} behavior of Rutherford scattering has for the nucleus in an atom. Consequently we would very much like to extend our range in P_T well beyond 9 GeV/c so that we can study the flavor dependence of constituent scattering. With protons incident the Tevatron (minimal Tevatron) allows us to extend our P_T range beyond 12 GeV/c to 18 GeV/c (16 GeV/c). The improvement with pions incident (at 0.4 times the proton energy) is particularly important for studies of flavor dependence: from 7 to 11 GeV/c (10 GeV/c). For our correlation measurements the Tevatron (minimal Tevatron) allows us to detect pairs out to P_T's of 14 GeV/c on 14 GeV/c (12 GeV/c on 12 GeV/c)! Note, detecting singles and pairs in the same apparatus clarifies some of the 'trigger bias' problems that have frustrated many theoretical attempts to understand high P_T hadron spectra on the basis of constituent models.